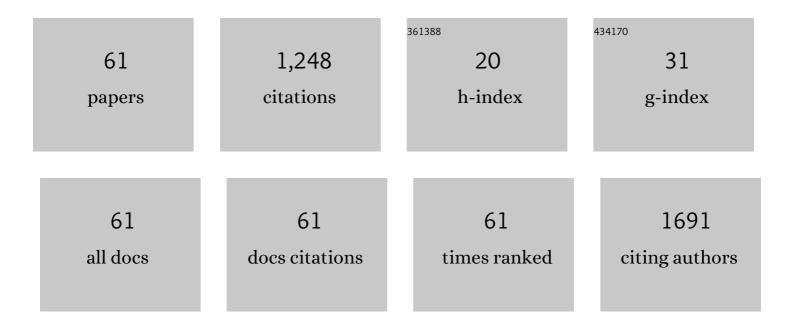
List of Publications by Year in descending order

Source: https://exaly.com/author-pdf/5636174/publications.pdf Version: 2024-02-01



HVO-LIN KANC

#	Article	IF	CITATIONS
1	Combined hepatocellular cholangiocarcinoma: LI-RADS v2017 categorisation for differential diagnosis and prognostication on gadoxetic acid-enhanced MR imaging. European Radiology, 2019, 29, 373-382.	4.5	89
2	Clinical Feasibility of 3-Dimensional Magnetic Resonance Cholangiopancreatography Using Compressed Sensing. Investigative Radiology, 2017, 52, 612-619.	6.2	66
3	Quantitative Assessment of Liver Function by Using Gadoxetic Acid–enhanced MRI: Hepatocyte Uptake Ratio. Radiology, 2019, 290, 125-133.	7.3	59
4	LI-RADS Version 2017 versus Version 2018: Diagnosis of Hepatocellular Carcinoma on Gadoxetate Disodium–enhanced MRI. Radiology, 2019, 292, 655-663.	7.3	55
5	Assessment of Malignant Potential in Intraductal Papillary Mucinous Neoplasms of the Pancreas: Comparison between Multidetector CT and MR Imaging with MR Cholangiopancreatography. Radiology, 2016, 279, 128-139.	7.3	54
6	Reproducibility of ultrasound attenuation imaging for the noninvasive evaluation of hepatic steatosis. Ultrasonography, 2020, 39, 121-129.	2.3	51
7	Preoperative CT Classification of the Resectability of Pancreatic Cancer: Interobserver Agreement. Radiology, 2019, 293, 343-349.	7.3	46
8	Gadoxetate-enhanced MRI Features of Proliferative Hepatocellular Carcinoma Are Prognostic after Surgery. Radiology, 2021, 300, 572-582.	7.3	45
9	Prognostic value of MRI in assessing extramural venous invasion in rectal cancer: multi-readers' diagnostic performance. European Radiology, 2019, 29, 4379-4388.	4.5	41
10	Virtual monoenergetic dual-layer, dual-energy CT enterography: optimization of keV settings and its added value for Crohn's disease. European Radiology, 2018, 28, 2525-2534.	4.5	39
11	LI-RADS treatment response categorization on gadoxetic acid-enhanced MRI: diagnostic performance compared to mRECIST and added value of ancillary features. European Radiology, 2020, 30, 2861-2870.	4.5	37
12	GRASE Revisited: breath-hold three-dimensional (3D) magnetic resonance cholangiopancreatography using a Gradient and Spin Echo (GRASE) technique at 3T. European Radiology, 2018, 28, 3721-3728.	4.5	32
13	High Acceleration Three-Dimensional T1-Weighted Dual Echo Dixon Hepatobiliary Phase Imaging Using Compressed Sensing-Sensitivity Encoding: Comparison of Image Quality and Solid Lesion Detectability with the Standard T1-Weighted Sequence. Korean Journal of Radiology, 2019, 20, 438.	3.4	32
14	Contrast-enhanced US with Sulfur Hexafluoride and Perfluorobutane for the Diagnosis of Hepatocellular Carcinoma in Individuals with High Risk. Radiology, 2020, 297, 108-116.	7.3	32
15	CT/MRI and CEUS LI-RADS Major Features Association with Hepatocellular Carcinoma: Individual Patient Data Meta-Analysis. Radiology, 2022, 302, 326-335.	7.3	32
16	Liver fibrosis staging with a new 2D-shear wave elastography using comb-push technique: Applicability, reproducibility, and diagnostic performance. PLoS ONE, 2017, 12, e0177264.	2.5	31
17	Initial M Staging of Rectal Cancer: FDG PET/MRI with a Hepatocyte-specific Contrast Agent versus Contrast-enhanced CT. Radiology, 2020, 294, 310-319.	7.3	31
18	Quantitative contrast-enhanced US helps differentiating neoplastic vs non-neoplastic gallbladder polyps. European Radiology, 2019, 29, 3772-3781.	4.5	24

#	Article	IF	CITATIONS
19	Microvascular Flow Imaging of Residual or Recurrent Hepatocellular Carcinoma after Transarterial Chemoembolization: Comparison with Color/Power Doppler Imaging. Korean Journal of Radiology, 2019, 20, 1114.	3.4	22
20	Prospective Validation of Intra- and Interobserver Reproducibility of a New Point Shear Wave Elastographic Technique for Assessing Liver Stiffness in Patients with Chronic Liver Disease. Korean Journal of Radiology, 2017, 18, 926.	3.4	21
21	Role of Contrast-Enhanced Ultrasound as a Second-Line Diagnostic Modality in Noninvasive Diagnostic Algorithms for Hepatocellular Carcinoma. Korean Journal of Radiology, 2021, 22, 354.	3.4	21
22	Joint segmentation and classification of hepatic lesions in ultrasound images using deep learning. European Radiology, 2021, 31, 8733-8742.	4.5	21
23	Clinical Feasibility of Gadoxetic Acid–Enhanced Isotropic High-Resolution 3-Dimensional Magnetic Resonance Cholangiography Using an Iterative Denoising Algorithm for Evaluation of the Biliary Anatomy of Living Liver Donors. Investigative Radiology, 2019, 54, 103-109.	6.2	20
24	Switching Monopolar No-Touch Radiofrequency Ablation Using Octopus Electrodes for Small Hepatocellular Carcinoma: A Randomized Clinical Trial. Liver Cancer, 2021, 10, 72-81.	7.7	19
25	Can quantitative iodine parameters on DECT replace perfusion CT parameters in colorectal cancers?. European Radiology, 2018, 28, 4775-4782.	4.5	18
26	Diagnosis and Surveillance of Incidental Pancreatic Cystic Lesions: 2017 Consensus Recommendations of the Korean Society of Abdominal Radiology. Korean Journal of Radiology, 2019, 20, 542.	3.4	18
27	Additional value of contrast-enhanced ultrasound (CEUS) on arterial phase non-hyperenhancement observations (≥ 2Âcm) of CT/MRI for high-risk patients: focusing on the CT/MRI LI-RADS categories LR-3 and LR-4. Abdominal Radiology, 2020, 45, 55-63.	2.1	18
28	Clinical Feasibility of Abbreviated Magnetic Resonance With Breath-Hold 3-Dimensional Magnetic Resonance Cholangiopancreatography for Surveillance of Pancreatic Intraductal Papillary Mucinous Neoplasm. Investigative Radiology, 2020, 55, 262-269.	6.2	15
29	Comparison of four different Shear Wave Elastography platforms according to abdominal wall thickness in liver fibrosis evaluation: a phantom study. Medical Ultrasonography, 2019, 21, 22.	0.8	15
30	Impact of Reference Standard on CT, MRI, and Contrast-enhanced US LI-RADS Diagnosis of Hepatocellular Carcinoma: A Meta-Analysis. Radiology, 2022, 303, 544-545.	7.3	15
31	Value of virtual monochromatic spectral image of dual-layer spectral detector CT with noise reduction algorithm for image quality improvement in obese simulated body phantom. BMC Medical Imaging, 2019, 19, 76.	2.7	14
32	Additional value of contrast-enhanced ultrasonography for fusion-guided, percutaneous biopsies of focal liver lesions: prospective feasibility study. Abdominal Radiology, 2018, 43, 3279-3287.	2.1	13
33	Clinical utility of real-time ultrasound-multimodality fusion guidance for percutaneous biopsy of focal liver lesions. European Journal of Radiology, 2018, 103, 76-83.	2.6	13
34	Prospective Validation of Repeatability of Shear Wave Dispersion Imaging for Evaluation of Non-alcoholic Fatty Liver Disease. Ultrasound in Medicine and Biology, 2019, 45, 2688-2696.	1.5	13
35	Evaluation of LI-RADS Version 2018 Treatment Response Algorithm for Hepatocellular Carcinoma in Liver Transplant Candidates: Intraindividual Comparison between CT and Hepatobiliary Agent–enhanced MRI. Radiology, 2021, 299, 336-345.	7.3	13
36	Diagnostic criteria of perfluorobutane-enhanced ultrasonography for diagnosing hepatocellular carcinoma in high-risk individuals: how is late washout determined?. Ultrasonography, 2022, 41, 530-542.	2.3	13

#	Article	IF	CITATIONS
37	Replacing single-view mediolateral oblique (MLO) digital mammography (DM) with synthesized mammography (SM) with digital breast tomosynthesis (DBT) images: Comparison of the diagnostic performance and radiation dose with two-view DM with or without MLO-DBT. European Journal of Radiology, 2016, 85, 2042-2048.	2.6	12
38	Diagnostic Performance of 2018 KLCA-NCC Practice Guideline for Hepatocellular Carcinoma on Gadoxetic Acid-Enhanced MRI in Patients with Chronic Hepatitis B or Cirrhosis: Comparison with LI-RADS Version 2018. Korean Journal of Radiology, 2021, 22, 1066.	3.4	12
39	Does Establishing a Safety Margin Reduce Local Recurrence in Subsegmental Transarterial Chemoembolization for Small Nodular Hepatocellular Carcinomas?. Korean Journal of Radiology, 2015, 16, 1068.	3.4	11
40	Sub-millisievert CT colonography: effect of knowledge-based iterative reconstruction on the detection of colonic polyps. European Radiology, 2018, 28, 5258-5266.	4.5	10
41	Additional values of highâ€resolution gadoxetic acidâ€enhanced MR cholangiography for evaluating the biliary anatomy of living liver donors: Comparison with <i>T</i> ₂ â€weighted MR cholangiography and conventional gadoxetic acidâ€enhanced MR cholangiography. Journal of Magnetic Resonance Imaging, 2018, 47, 152-159.	3.4	10
42	Gastrointestinal tract complications after hepatic radiofrequency ablation: CT prediction for major complications. Abdominal Radiology, 2018, 43, 583-592.	2.1	8
43	Synergistic Effects of Pulsed Focused Ultrasound and a Doxorubicin-Loaded Microparticle–Microbubble Complex in a Pancreatic Cancer Xenograft Mouse Model. Ultrasound in Medicine and Biology, 2020, 46, 3046-3058.	1.5	8
44	Quantitative evaluation of posterior talar subluxation in posterior malleolar fractures: A preliminary study. Injury, 2020, 51, 1669-1675.	1.7	8
45	Ultrasound-guided transient elastography and two-dimensional shear wave elastography for assessment of liver fibrosis: emphasis on technical success and reliable measurements. Ultrasonography, 2021, 40, 217-227.	2.3	8
46	Perfluorobutane-enhanced ultrasonography with a Kupffer phase: improved diagnostic sensitivity for hepatocellular carcinoma. European Radiology, 2022, 32, 8507-8517.	4.5	8
47	T2* Mapping from Multi-Echo Dixon Sequence on Gadoxetic Acid-Enhanced Magnetic Resonance Imaging for the Hepatic Fat Quantification: Can It Be Used for Hepatic Function Assessment?. Korean Journal of Radiology, 2017, 18, 682.	3.4	7
48	Comparisons between image quality and diagnostic performance of 2D- and breath-hold 3D magnetic resonance cholangiopancreatography at 3T. European Radiology, 2021, 31, 8399-8407.	4.5	6
49	Transabdominal Ultrasound for Follow-Up of Incidentally Detected Low-Risk Pancreatic Cysts: A Prospective Multicenter Study. American Journal of Roentgenology, 2021, 216, 1521-1529.	2.2	6
50	Addition of Reliability Measurement Index to Point Shear Wave Elastography: Prospective Validation via Diagnostic Performance and Reproducibility. Ultrasound in Medicine and Biology, 2019, 45, 1594-1602.	1.5	5
51	Intra-individual comparison of dual portal venous phases for non-invasive diagnosis of hepatocellular carcinoma at gadoxetic acid–enhanced liver MRI. European Radiology, 2021, 31, 824-833.	4.5	5
52	Virtual noncontrast images derived from dual-energy CT for assessment of hepatic steatosis in living liver donors. European Journal of Radiology, 2021, 139, 109687.	2.6	5
53	Reduction of olecranon fractures with no or minimal dorsal cortex comminution based on the contour of the posterior ulnar cortex: does it restore the greater sigmoid notch?. Archives of Orthopaedic and Trauma Surgery, 2022, 142, 2215-2224.	2.4	4
54	Usefulness of contrast-enhanced ultrasound using perfluorobutanecontaining microbubbles as a planning for percutaneous biopsies of focal hepatic lesions: a prospective feasibility study. Medical Ultrasonography, 2019, 21, 109.	0.8	4

#	Article	IF	CITATIONS
55	Differentiation of intra-abdominal desmoid tumor from peritoneal seeding based on CT and/or 18F-FDG PET-CT in patients with history of cancer surgery. Abdominal Radiology, 2020, 45, 2647-2655.	2.1	3
56	Prediction of prognosis and resectability using MR imaging, clinical, and histopathological findings in patients with perihilar cholangiocarcinoma. Abdominal Radiology, 2021, 46, 4159-4169.	2.1	3
57	Additional value of superb microvascular imaging of ultrasound examinations to evaluate focal liver lesions. European Journal of Radiology, 2022, 152, 110332.	2.6	3
58	Differentiation between small (< 4.5 cm) true subepithelial tumors and ectopic pancreas in the small bowel on computed tomography enterography. European Radiology, 2021, , 1.	4.5	2
59	Contrast-Enhanced Ultrasound for Focal Hepatic Lesions. Ultrasound Quarterly, 2020, 36, 224-234.	0.8	1
60	Prediction of residual tumor and overall survival after first-line surgery in patients with pancreatic ductal adenocarcinoma using preoperative magnetic resonance imaging findings. Acta Radiologica, 2021, , 028418512199999.	1.1	1
61	Pancreatic Tumors. Medical Radiology, 2017, , 491-525.	0.1	0